



Associations with Retinal Pigment Epithelium Thickness Measures in a Large Cohort

Results from the UK Biobank

Fang Ko, MD,¹ Paul J. Foster, PhD, FRCOphth,¹ Nicholas G. Strouthidis, PhD, FRCOphth,¹ Yusrah Shweikh, MBChB, MRes,¹ Qi Yang, PhD,² Charles A. Reisman, MS,² Zaynah A. Muthy, BSc,¹ Usha Chakravarthy, MD, PhD,³ Andrew J. Lotery, MD, FRCOphth,⁴ Pearse A. Keane, MD, MRCOphth,¹ Adnan Tufail, MD, FRCOphth,¹ Carlota M. Grossi, PhD,¹ Praveen J. Patel, MD, FRCOphth,¹ on behalf of the UK Biobank Eye & Vision Consortium*

Purpose: To describe associations of ocular and systemic factors with retinal pigment epithelium (RPE)–Bruch’s membrane (BM) complex thickness as measured by spectral-domain (SD) optical coherence tomography (OCT).

Design: Multisite community-based study. This research has been conducted using the UK Biobank Resource.

Participants: Sixty-seven thousand three hundred eighteen people 40 to 69 years old received questionnaires, physical examination, and eye examination, including macular SD OCT. Systematic selection process identified 34 652 eyes with high-quality SD OCT images from normal individuals for analysis.

Methods: We included people with no self-reported ocular disease, diabetes, or neurologic disorders; visual acuity of $\geq 20/25$ or better; refraction between -6 diopters (D) to 6 D, and IOP of 6 to 21 mmHg. Only high-quality, well-centered SD OCT images with central, stable fixation were included. Descriptive statistics, *t* tests, and regression analyses were performed. Multivariate regression modeling was used to adjust for covariates and to identify relationships between RPE–BM thickness and ocular and systemic features.

Main Outcome Measures: Retinal pigment epithelium–BM thickness, as measured by SD OCT segmentation using Topcon Advanced Boundary Segmentation at 9 Early Treatment of Diabetic Retinopathy Study subfields.

Results: Mean RPE–BM thickness was 26.3 μm (standard deviation, 4.8 μm) at central subfield. Multivariate regression with age stratification showed that RPE thinning became apparent after age 45 years. Among those aged ≤ 45 , RPE–BM was significantly thicker among those of black or mixed/other race (+3.61 μm and +1.77 μm vs. white, respectively; $P < 0.001$) and higher hyperopia (+0.4 $\mu\text{m}/\text{D}$; $P < 0.001$), but not for other variables considered. Among those age > 45 , RPE–BM was significantly thinner with older age (-0.10 $\mu\text{m}/\text{year}$; $P < 0.001$), Asian ethnicity (-0.45 μm vs. white; $P = 0.02$), taller height (-0.02 $\mu\text{m}/\text{cm}$; $P < 0.001$), higher IOP (-0.03 $\mu\text{m}/\text{mmHg}$; $P < 0.001$), and regular smoking (-0.27 μm vs. nonsmokers; $P = 0.02$). In contrast, RPE–BM was significantly thicker among black or mixed/other race (+3.29 μm and +0.81 μm vs. white, respectively; $P < 0.001$) and higher hyperopia (+0.28 $\mu\text{m}/\text{D}$; $P < 0.001$). There was no significant association with sex or Chinese ethnicity.

Conclusions: We describe novel findings of RPE–BM thickness in normal individuals, a structure that varies with age, ethnicity, refraction, IOP, and smoking. The significant association with IOP is especially interesting and may have relevance for the etiology of glaucoma, while the association between age and smoking may have relevance for the etiology of age-related macular degeneration. *Ophthalmology* 2016;■:1–13 © 2016 by the American Academy of Ophthalmology



*Supplemental material is available at www.aaojournal.org.

Optical coherence tomography (OCT) is an imaging method that allows unprecedented in vivo study of the macula.^{1,2} Advances in both hardware and software now facilitate resolution and segmentation of optical reflectivity boundaries thought to represent retinal sublayers with resolution of

4 to 6 μm including, but not limited to, the retinal pigment epithelium (RPE).^{3,4} The RPE plays an important role in metabolic activity in the retina and is critical in visual function.⁵ Failure of RPE function is involved in blinding diseases such as age-related macular degeneration, the

leading cause of blindness among white people 65 years of age and older.^{6–10}

Despite its importance, little is known about the normal distribution of RPE thickness in the nondiseased state. Postmortem histologic studies suggest increases in RPE autofluorescence and Bruch's membrane (BM) thickness with age.^{11–13} A small histologic study of 18 maculae showed mean RPE thickness of 14.1 μm and mean BM thickness of 4.7 μm at the foveal center.¹⁴ Histologic studies are limited in that they are postmortem or use enucleated eyes and can be affected easily by artifact during handling of tissue. In vivo investigations have been made with spectral-domain (SD) optical coherence tomography (OCT), but sample sizes remain small. A study of 25 healthy individuals showed mean RPE–BM complex thickness of 22.7 μm at the central subfield and also suggested that the thickness increases with age.¹⁵ Recently, a database of SD OCT images was created, but includes images from only 115 healthy people and 269 with macular degeneration.¹⁶

The UK Biobank is a community-based cohort study in the United Kingdom and includes SD OCT image acquisitions from 67 321 participants in addition to systemic biomarkers and laboratory testing. To our knowledge, this is the largest study of retinal imaging yet undertaken. Our aim was to determine the distribution of the RPE among individuals who report no ocular disease and to examine variation with age, gender, race, refraction (between 6 and -6 diopters [D]), intraocular pressure (IOP; 6–21 mmHg), smoking status, blood pressure (BP), and body mass index (BMI).

Methods

The UK Biobank is a 22-site community-based cohort study of 502 656 noninstitutionalized civilian United Kingdom residents 40 to 69 years of age who were registered with the National Health Service. Health questionnaire and biological samples (blood, urine, and saliva) were collected from all participants. Participants identified their own race as either white, Chinese, Asian (in this cultural context, most were of Indian descent, but also included Pakistani and Bangladeshi subjects, as well as others), black, or mixed or other. People were asked whether they were current tobacco smokers; possible answers were no, occasional, or most or all days. Those who answered no to current smoking but who said they previously smoked occasionally or most or all days were considered former smokers. Health examination included BP and BMI. Eye data, including visual acuity, autorefractometry, Goldmann-corrected IOP, and cornea-corrected IOP (Ocular Response Analyzer; Reichert, Depew, NY) were collected from 133 668 people. Retinal OCT measurements were acquired among the latter half of these; in total, 67 318 people underwent retinal OCT imaging. The North West Multi-center Research Ethics Committee approved the study (reference no., 06/MRE08/65), in accordance with the tenets of the Declaration of Helsinki. Detailed information about the study is available at the UK Biobank web site (www.ukbiobank.ac.uk).

Spectral-Domain Optical Coherence Tomography Imaging Protocol

Spectral-domain OCT imaging was performed using the Topcon 3D OCT 1000 Mk2 (Topcon, Inc, Oakland, NJ) after visual acuity,

autorefractometry, and IOP measurements were obtained. Image acquisition was performed under mesopic conditions, without pupillary dilation, using the 3-dimensional macular volume scan (512 horizontal A-scans/B-scans; 128 B-scans in a 6 \times 6-mm raster pattern). The protocol specified that the right eye should be imaged first, but in 44 participants, the left eye was imaged first.

Analysis of Macular Thickness

All SD OCT images were stored as .fds image files on the UK Biobank supercomputers in Oxford, United Kingdom, with no prior analysis of macular thickness. Version 1.6.1.1 of the Topcon Advanced Boundary Segmentation (TABS) algorithm was used to segment the inner and outer retinal surfaces automatically.¹⁷ Quality control measures included the image quality score, the internal limiting membrane (ILM) indicator, a validity count, and motion indicators. The image quality score gives a measure of signal strength for the scan, whereas the ILM indicator is a measure of the minimum localized edge strength around the ILM boundary across the entire volume. The ILM indicator is useful for identifying blinks, scans that contain regions of severe signal attenuation, segmentation errors, or a combination thereof. The validity count indicator is used to identify scans with a significant degree of clipping in the OCT scan's z-axis dimension. The motion indicators use both the nerve fiber layer (NFL) and full retinal thicknesses, from which Pearson correlations and absolute differences between the thickness data from each set of consecutive B-scans are calculated. The lowest correlation and the highest absolute difference in a scan serve as the resulting indicator scores. This last group of indicators identifies blinks, eye-motion artifacts, and segmentation failures. It should be noted that the various indicators, including the image quality score, tend to be highly correlated with one another.

Defining the Retinal Pigment Epithelium–Bruch's Membrane Complex on Spectral-Domain Optical Coherence Tomography

The TABS segmentation algorithm was used to delineate the RPE–BM complex. This slab of tissue on the OCT is represented by a thick hyperreflective band that lies on the outer aspect of the retina. The algorithm places a boundary on the inner and outer surfaces of this band, and the distance between these 2 boundary lines represents the thickness of RPE–BM complex.¹⁸ Specifically, the inner boundary for the RPE–BM band corresponds to the TABS photoreceptor outer segment–RPE boundary, and the outer boundary is delineated by the BM–choroid boundary. [Figure 1](#) shows an SD OCT line scan from the UK Biobank dataset with and without RPE segmentation lines.

Inclusion and Exclusion Criteria

The RPE–BM complex thickness values from the eyes of all patients who underwent SD OCT as part of the UK Biobank were used as a starting point for analysis. Patients were excluded from the analysis if they withdrew consent, had poor SD OCT signal strength and missing thickness values from any Early Treatment Diabetic Retinopathy Study subfield, image quality score less than 45, poor centration certainty, or poor segmentation certainty using TABS software (poorest 20% of images excluded based on each of the segmentation indicators). This led to the identification of the subset of patients with good-quality, well-centered images and central, stable fixation during the OCT scan. Patients with high refractive error of more than 6 D or less than -6 D, visual acuity worse than 20/30, self-reported glaucoma, IOP of 22 mmHg or

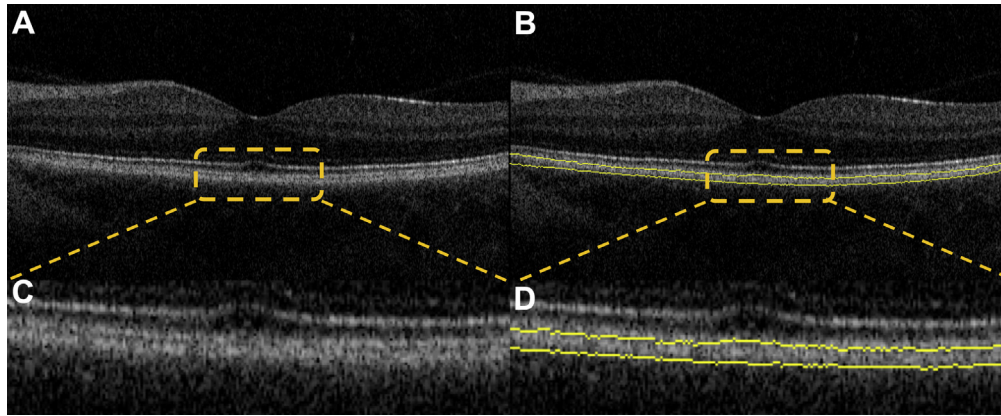


Figure 1. Spectral-domain optical coherence tomography images showing representative retinal pigment epithelium–Bruch’s membrane complex segmentation results. **A**, Foveal B-scan image from an accepted volume. **B**, Retinal pigment epithelium–Bruch’s membrane complex segmentations for the foveal B-scan image. **C** and **D**, Magnified views of (**A**) and (**B**), respectively.

more or 5 mmHg or less, self-reported ocular disorders, diabetes, or neurodegenerative disease were excluded. Finally, if both eyes of a patient were eligible for inclusion in this analysis, one eye was chosen at random using STATA software (StataCorp LP, College Station, TX) for randomization (Fig 2).

A subset of images was selected for manual grading, focusing on those at the extremes of macular thickness after inclusion and exclusion criteria were applied. The selection of scans for manual analysis was the same as that adopted for previous work analyzing macular thickness in the UK Biobank cohort.¹⁹

Statistical Analysis

Statistical analyses were performed using STATA software version 12.0. Means, standard errors, standard deviations, and 95% confidence intervals were calculated for the RPE–BM complex thickness among all participants, subsets of different demographic variables, as well as ocular and systemic variables. If a trend was noted, then linear regression analysis was performed. Unpaired *t* tests were performed to compare means. Values were considered significant if the *P* value was less than 0.05.

Results

Of the 67 321 people who underwent SD OCT macular imaging, 51 987 had high-quality images. Of these, 34 752 people had refractive error within 6 D of emmetropia, vision of 20/30 or better, no self-report of glaucoma or missing IOP measurement, no self-reported ocular disorders, and no neurologic disease or diabetes, and thus were eligible for inclusion in the analysis (Fig 2). A further 288 patients were excluded on the basis of the manual assessment of images. This left 34 464 eyes of 34 464 people included in the analysis. The mean age was 56.0 years, with a slightly higher number of women (53.7%) than men. The mean height was shorter among women (163 cm) than men (176 cm; $P < 0.001$). Most participants were white, with 129 Chinese participants, 898 Asian participants, 974 black participants, and 795 participants of mixed or other race or ethnicity. There were more left eyes than right. Mean visual acuity was -0.04 logarithm of the minimum angle of resolution, mean refraction was -0.05 D, and mean IOP was 15 mmHg (Table 1).

A histogram of RPE–BM complex thickness (Fig 3A) shows a mean thickness of 26.3 μm (standard deviation, 4.8 μm) in the central subfield. Figure 3B shows the mean RPE–BM complex thickness in different Early Treatment Diabetic Retinopathy Study subfields, with nasal and temporal subfields significantly thicker than superior or inferior subfields ($P < 0.001$). The thickest subfield was the inner nasal subfield. Results remained consistent for women and men (Fig 3C). Furthermore, women had thicker RPE–BM complexes in the central and inner superior subfields ($P < 0.001$), whereas men seemed to have thicker RPE–BM complexes in all other subfields ($P < 0.001$) except the inner inferior subfield, which was not significant.

Figure 4A shows mean central RPE–BM complex thickness by age. Central macular subfield RPE–BM complex thickness showed no significant changes between 40 and 45 years of age; however, after age 46 years, mean thickness declined steadily at a rate of 0.10 $\mu\text{m}/\text{year}$ ($P < 0.001$). A similar trend was evident among all subfields (Fig 4B, C), with linear regression showing no significant changes from 40 to 45 years of age and a negative slope after age 46 years of age in every subfield ($P < 0.001$; Table S1, available at www.aaojournal.org). At all ages, nasal and temporal subfields were significantly thicker than superior and inferior subfields, with nasal subfields being the thickest (Fig 4B, C).

When the RPE–BM complex thickness was compared among different races, black race showed significantly greater thickness at every subfield (Fig S1, available at www.aaojournal.org). White, Chinese, and Asian persons showed similar central RPE–BM complex thickness. When RPE–BM complex thickness was analyzed by refraction, hyperopes showed significantly thicker central RPE–BM, with linear regression estimating an increase of 0.2 $\mu\text{m}/\text{D}$ (Fig 5A). A similar trend was seen for all subfields (Fig 5B, C; Table S2, available at www.aaojournal.org).

To determine whether race or ethnicity and refraction are potential confounders, RPE–BM complex thicknesses were plotted for both variables (Fig 6; Chinese and mixed or other race or ethnicity were excluded because of the small numbers in the race or ethnicity and refraction subgroups). At the central subfield, black race continued to show the greatest RPE–BM complex thickness, with Asian and white race demonstrating similar

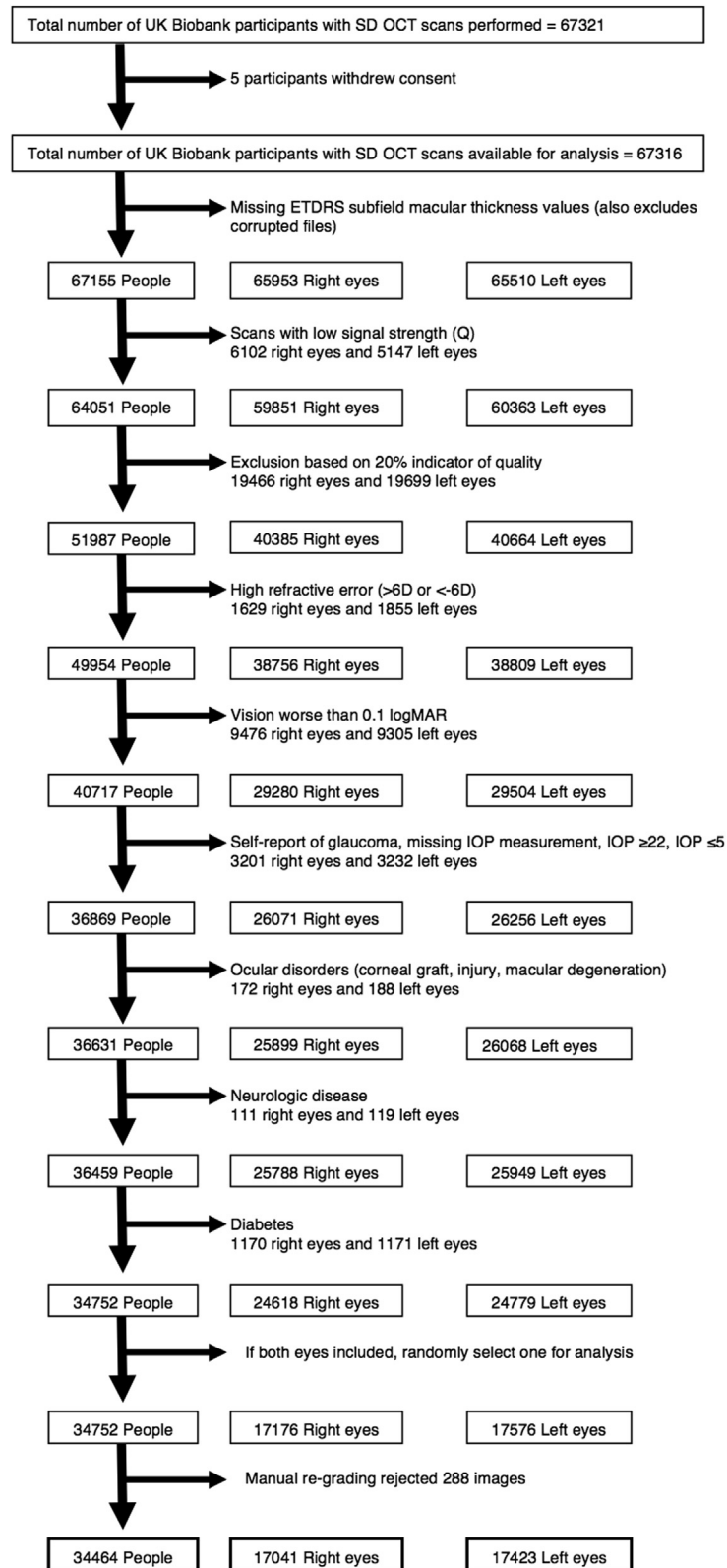


Figure 2. Flowchart showing retinal pigment epithelium inclusion and exclusion criteria. D = diopter; ETDRS = Early Treatment Diabetic Retinopathy Study; IOP = intraocular pressure; logMAR = logarithm of the minimum angle of resolution; OCT = optical coherence tomography; SD = spectral-domain.

Table 1. Basic Demographics

	Estimate (95% Confidence Interval)	No. or Standard Deviation (Total n = 34 726)
Mean age (yrs)	56.0 (55.9–56.1)	SD, 8.2
Female gender (%)	53.7 (53.2–54.2)	n = 18 615 (16 137 men)
Mean height (cm)	169.2 (169.1–169.3)	SD, 9.2
Women	163.1 (163.0–163.2)	SD, 6.3
Men	176.3 (176.2–176.4)	SD, 6.8
Race/Ethnicity (%)		
White	91.8 (91.5–92.1)	n = 31 442
Chinese	0.4 (0.3–0.4)	n = 129
Asian	2.6 (2.5–2.8)	n = 898
Black	2.8 (2.7–3.0)	n = 974
Mixed/other	2.3 (2.2–2.5)	n = 795
Right eye laterality (%)	49.4 (48.9–50.0)	n = 17 041 (17 423 left)
Mean visual acuity (logMAR)	−0.04 (−0.042 to −0.039)	SD, 0.157
Mean refraction	−0.05 (−0.07 to −0.03)	SD, 1.91
Mean IOP (Goldmann corrected)	15.0 (15.0–15.1)	SD, 3.0

IOP = intraocular pressure; logMAR = logarithm of the minimum angle of resolution; SD = standard deviation.

RPE–BM complex thicknesses. Among whites, there continued to be a trend toward increasing central RPE–BM complex thickness per 1-D increase in refraction; however, this effect was small compared with racial and ethnic differences. Among Asians and blacks, there was no trend in central RPE–BM complex thickness by refraction. The effects of ethnicity or race and refraction on RPE–BM complex thickness remained consistent for all subfields, with ethnicity or racial effects overshadowing that of increased mean RPE thickness with increased hyperopia (Fig S2, available at www.aaojournal.org).

The relationship between RPE–BM complex thickness and IOP is illustrated in Figure 7. In the central subfield, higher IOP was correlated with thinner RPE–BM complex thickness, with regression slope of $-0.08 \mu\text{m}$ per 1 mmHg ($P < 0.001$; Fig 7A). This trend was consistent across all subfields (Fig 7B, C).

A dose response with smoking status was not observed, but significant differences were detected between the different classes of smoking habit. Current smoking habit did not correlate with RPE–BM complex thickness (Table 2). Former smokers had significantly thinner RPE–BM complexes than nonsmokers (26.1 vs. 26.5 μm , respectively; $P < 0.001$) in the central subfield. Current smokers who classified themselves as regular smokers showed significantly thicker RPE–BM complexes as compared with nonsmokers at the inner temporal ($P = 0.003$), outer temporal ($P < 0.001$), outer superior ($P = 0.04$), outer nasal ($P < 0.001$), and outer inferior ($P < 0.001$) subfields. Current smokers were not significantly different from nonsmokers, regardless of whether they smoked occasionally or on most or all days, for inner superior, inner nasal, and inner inferior subfields, which showed the same trend (Table 2). Occasional smokers had significantly thicker RPE–BM complexes at the outer temporal ($P < 0.001$), outer superior ($P = 0.02$), outer nasal ($P < 0.001$), and outer inferior ($P < 0.001$) subfields (Table 2).

There is no significant association between systolic BP (Fig S3A and Table S3, available at www.aaojournal.org), diastolic BP (Fig S3B and Table S3, available at www.aaojournal.org), or BMI (Fig S4A and Table S4, available at www.aaojournal.org). Body mass index and race or ethnicity were considered together,

and again no association was identified (Fig S4B, available at www.aaojournal.org).

Because height and gender may be potential confounders, the 2 variables were examined separately and together (Fig S5 and Table S5A,B, available at www.aaojournal.org). When regression analysis was performed together for gender and height, changes in significance were noted at the central subfield, which remained significantly thicker among women, the inner inferior subfield, which lost statistical significance, and the inner inferior subfield, which became significantly thicker among men.

Variables found to be significant in univariate analysis were included in the multivariate regression modeling of central RPE–BM complex thickness (Table 3). The central subfield was chosen for analysis because it is the subfield with greatest clinical significance. Also, because of our findings of different effects of age before and after 45 years in single variable analysis, with no effect before 45 years of age and gradual thinning evident at age 46 years and older, separate models were performed for those 45 years of age and younger versus those older than 45 years. For those 45 years of age and younger, only race or ethnicity (black or mixed or other) and refraction were associated significantly with increased RPE–BM complex thickness (Table 3). In contrast, those older than 45 years showed RPE–BM complexes that were significantly thinner with older age ($-0.1 \mu\text{m}/\text{year}$; $P < 0.001$), Asian race ($-0.45 \mu\text{m}$ vs. white race; $P = 0.02$), taller height ($-0.02 \mu\text{m}/\text{cm}$; $P < 0.001$), higher IOP ($-0.03 \mu\text{m}/\text{mmHg}$; $P < 0.001$), higher myopia ($-0.28 \mu\text{m}/\text{D}$; $P < 0.001$), and regular smoking ($-0.27 \mu\text{m}$ compared with nonsmokers; $P = 0.02$). The central RPE–BM complex was thicker with black race or mixed or other race or ethnicity (3.29 μm and 0.81 μm compared with whites, respectively; $P < 0.001$). Female gender, Chinese race, and former or occasional smoking were not significant (Table 3).

Discussion

Using the largest known dataset of macular SD OCT measurements, we showed novel findings relating to RPE–BM

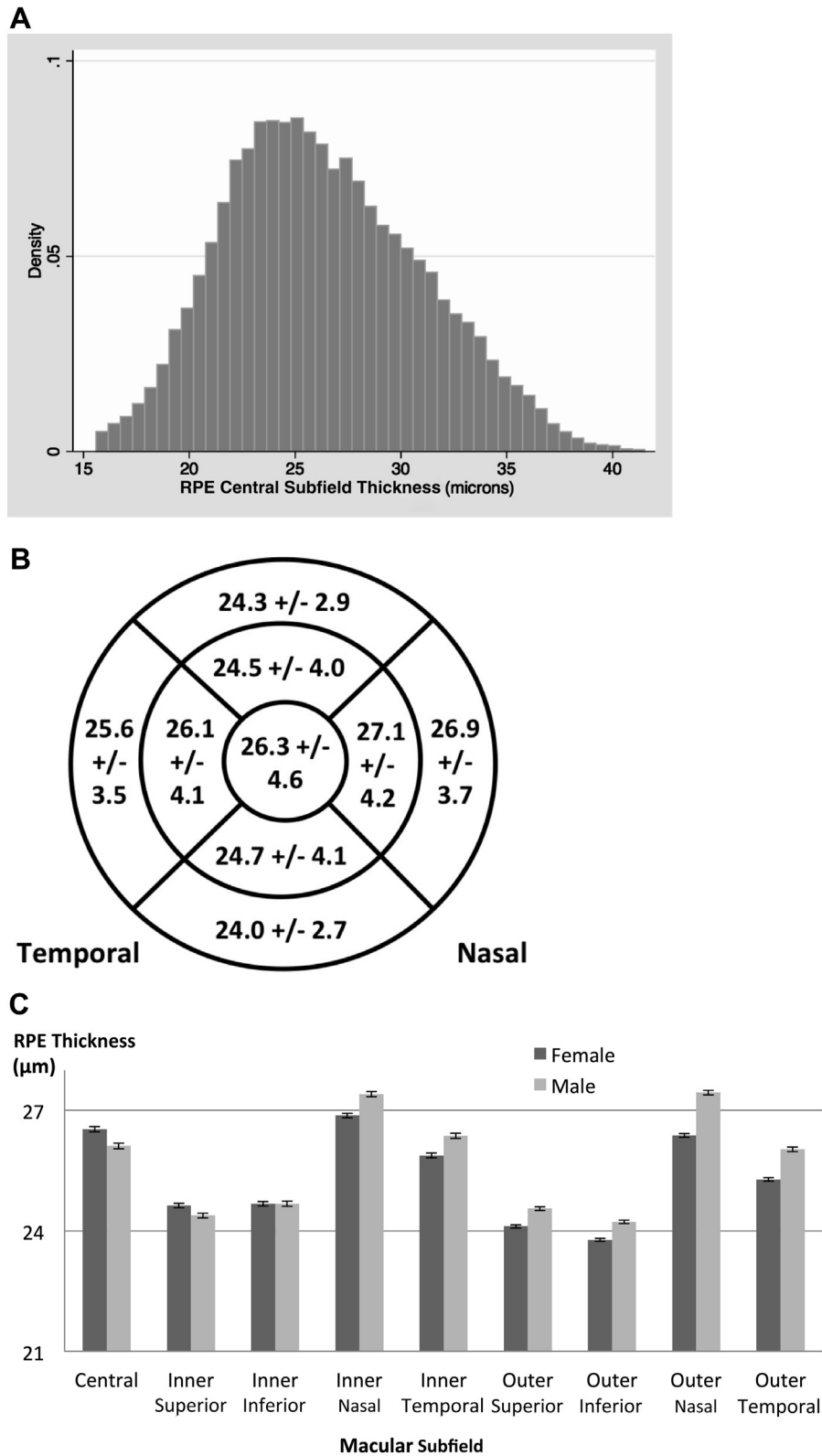


Figure 3. **A**, Histogram showing central retinal pigment epithelium (RPE) thickness (including Bruch's membrane). Mean, 26.34 μm ; standard error, 0.02 μm ; standard deviation, 4.80 μm . **B**, Diagram showing RPE thickness (including Bruch's membrane) at different locations. Data are mean \pm standard deviation (μm). $P < 0.001$ for t test of all subfields compared with central subfield. **C**, Bar graph showing RPE thickness (including Bruch's membrane) in women and men at different locations. Error bars represent 95% confidence intervals. $P < 0.001$ at all subfields except inner inferior ($P = 0.13$), t test of women versus men.

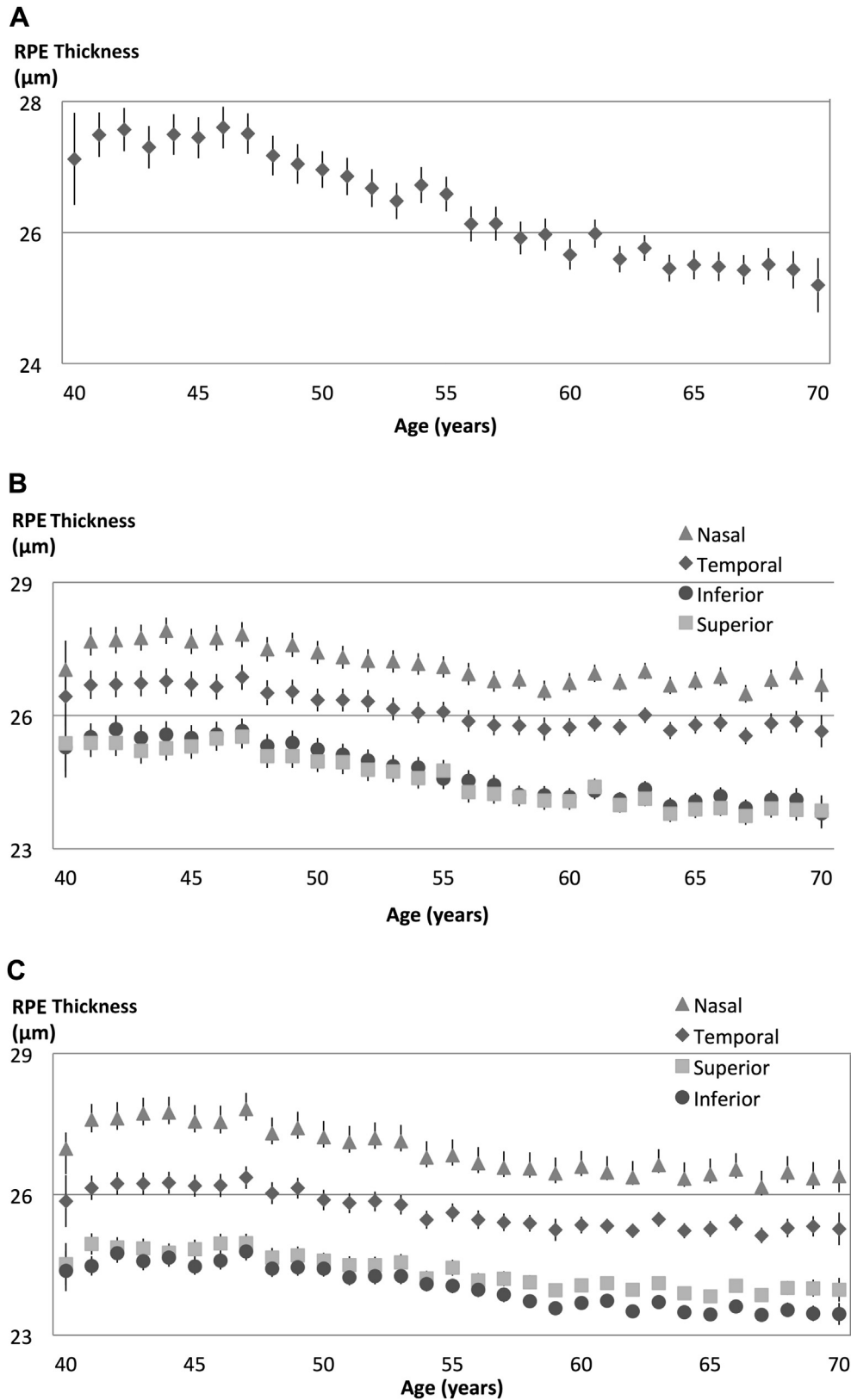


Figure 4. A, Graph showing the mean central retinal pigment epithelium (RPE) thickness (including Bruch's membrane) by age. Linear regression for ages 45 and younger, $27.3 + 0.004$ (per year), $P = 0.93$. Linear regression for ages 46 and older, $31.74 - 0.10$ (per year), $P < 0.001$. Error bars, 95% confidence interval. B, Graph showing the mean RPE thickness (including Bruch's membrane) of inner subfields by age. Error bars, 95% confidence interval. C, Graph showing the mean RPE thickness (including Bruch's membrane) of outer subfields by age. Error bars, 95% confidence interval.

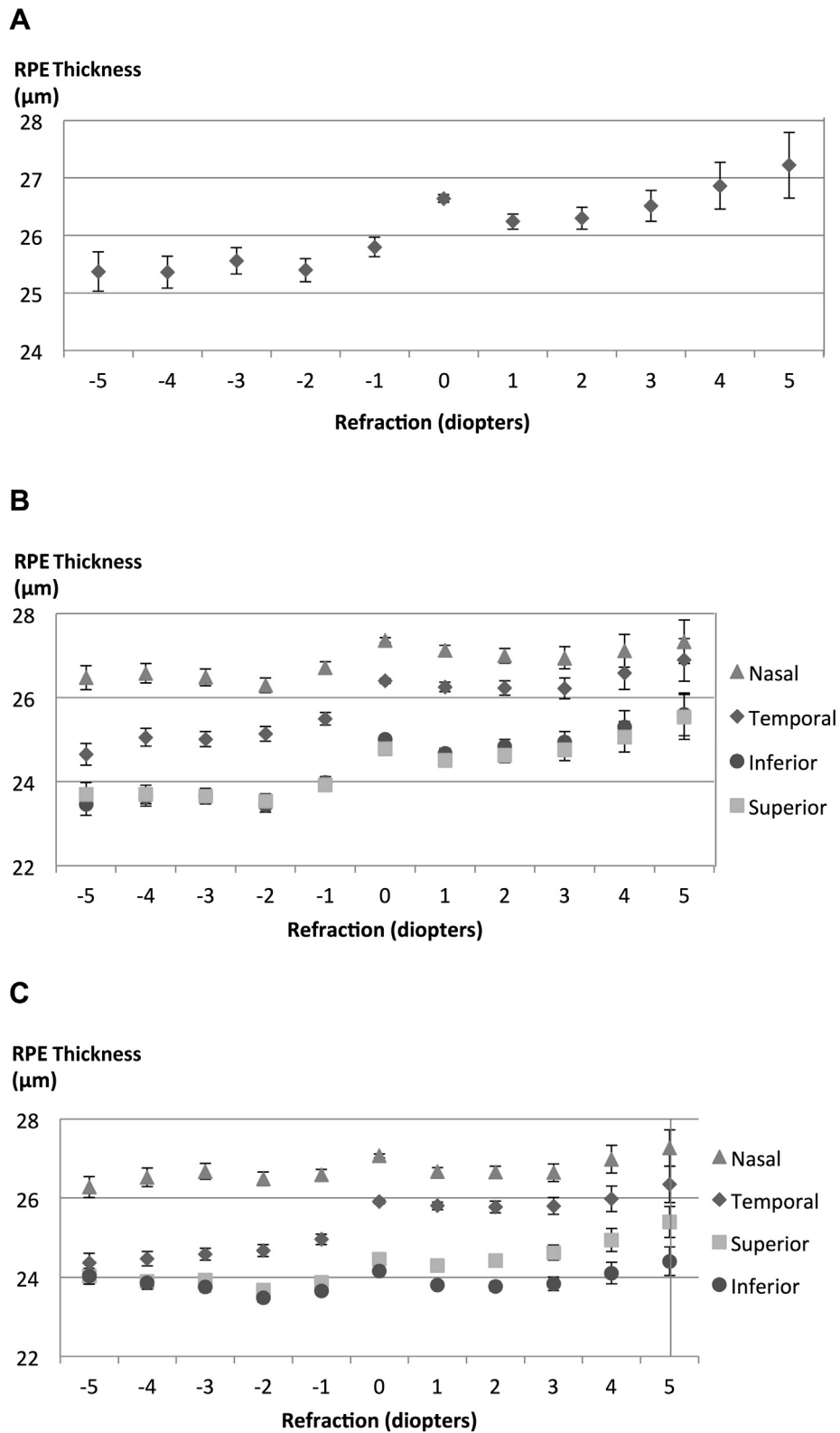


Figure 5. A, Graph showing the mean central retinal pigment epithelium (RPE) thickness (including Bruch's membrane) by refraction. Linear regression, $26.4 + 0.2$ (per 1 diopter), $P < 0.001$. Error bars, 95% confidence interval. B, Graph showing the mean RPE thickness (including Bruch's membrane) of inner subfields by refraction. Error bars, 95% confidence interval. C, Graph showing the mean RPE thickness (including Bruch's membrane) of outer subfields by refraction. Error bars, 95% confidence interval.

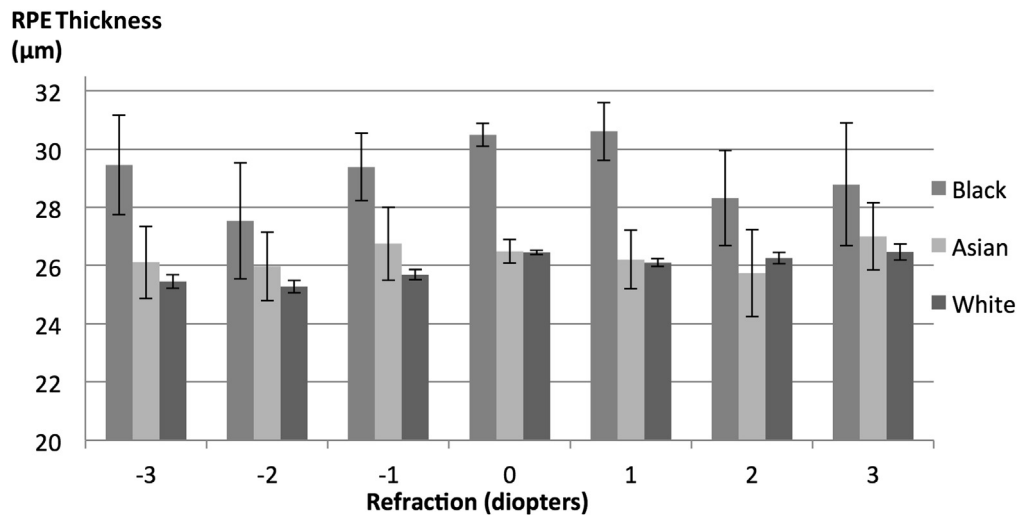


Figure 6. Bar graph showing the mean central retinal pigment epithelium (RPE) thickness (including Bruch's membrane) by race/ethnicity and refraction. Linear regression for white race/ethnicity = $26.15 + 0.21$ (per 1 diopter [D]), $P < 0.001$; Asian ethnicity = $26.39 + 0.11$ (per 1 D), $P > 0.49$; black race/ethnicity = $30.36 + 0.23$ (per 1 D), $P = 0.22$. Error bars, 95% confidence interval.

complex thickness and its distribution by demographic, ocular, and systemic indices. We showed that RPE–BM complex is significantly thicker in the nasal and temporal macular subfields as compared with the superior or inferior subfields, with the greatest thickness in the inner nasal subfield (Fig 3B). This remains true regardless of gender (Fig 3C), age (Fig 4), race (Fig S1, available at www.aaojournal.org), refractions (Fig 5), IOP (Fig 7), all BP values (Fig S3, available at www.aaojournal.org), and all levels of BMI (Fig S4, available at www.aaojournal.org). Our values of RPE–BM complex thickness are larger than those reported from histologic analyses¹⁴ by up to 4 to 5 μm . Most of this difference may be accounted for by the way the segmentation algorithm used in our study identified the inner RPE boundary and outer RPE–BM complex boundary. Both boundaries are placed by the algorithm on the hyporeflective side of the respective boundary edge. Therefore, this effectively adds an extra pixel to the thickness value, which on the 3-dimensional OCT-1000 Mark 2 system corresponds to 3.5 μm . This means that the fairest comparison with previous studies of histologic analyses would need to subtract 3.5 μm from the current study results. When this is done, the measurements become notably closer to those of previous studies (within 1–2 μm).

The RPE–BM complex becomes thinner with each year of age older than 46 years, decreasing 0.1 $\mu\text{m}/\text{year}$ (Fig 4A, Table 3). This trend persists for all subfields (Fig 4B, C; Table S1, available at www.aaojournal.org). Our findings are in contrast to those of other studies that indicated that RPE–BM complex thickness increases with age.^{15,20} However, the numbers included in at least 1 of these studies was too small to be conclusive.¹⁵ In the other study, numbers were marginally larger; but the age range was wider (18–81 years) and the proportion of people of comparable age as the participants included in the current study (40–69 years) was relatively small.²⁰ Although our study

controlled the analysis for gender, race was not adjusted for and this is a potential confounder, particularly because we found race or ethnicity to be associated significantly with RPE–BM complex thickness. Histologic studies show an increasing deposition of material in the basement membrane with age.^{11–13} The findings from our in vivo study suggested that the reductions in RPE–BM complex thickness that we observed with age are probably even greater. It is possible that measurements made on histologic examination may reflect focal changes, whereas OCT has the potential to provide averaged estimates of change within an entire section or subfield of the retina. Another possible explanation for our findings is that age-related loss of RPE cells may lead to remaining cells spreading horizontally to take up space freed by loss of neighboring cells. This process would lead to loss of vertical height of RPE cells with age and resultant reduced RPE–BM complex thickness with age. There is some support for attrition of the RPE cell layer with age.²¹ Histologic studies have shown spreading and reducing height of RPE cells, which implies a reducing density for a given area. However, there is insufficient evidence for RPE cell loss with age at present, making this explanation for our findings less likely. Men and women seemed to have different distribution of RPE–BM complex thickness, but these were no longer significant after controlling for other variables in multivariate regression modeling.

Black subjects had significantly thicker RPE–BM complexes on OCT compared with other races, approximately 3 to 4 μm (approximately 12%) more than whites and Asians (Table 3). This effect is unlikely to be associated with skin pigmentation, because there is no significant difference between Chinese and white subjects and possibly a trend in the opposite direction among Asian and white subjects. To our knowledge, this is the first time this finding has been demonstrated, and it may hold clues to the variable phenotypes of macular degeneration in different populations.²²

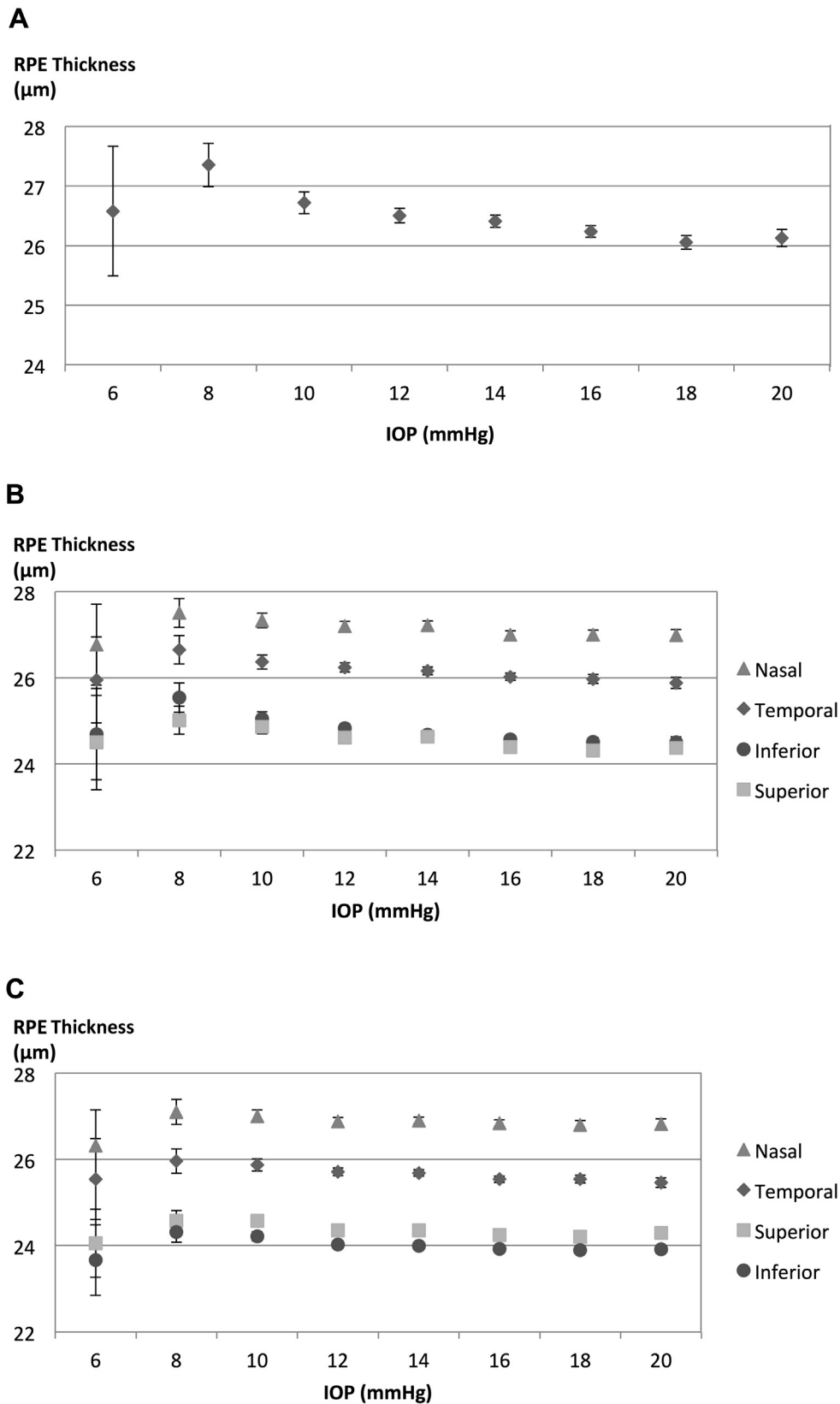


Figure 7. A, Graph showing the mean central retinal pigment epithelium (RPE) thickness (including Bruch's membrane) by intraocular pressure (IOP). Linear regression for IOP of 8 mmHg and more = $27.47 - 0.08$ (per 1 mmHg), $P < 0.001$. Error bars, 95% confidence interval. B, Graph showing the mean RPE thickness (including Bruch's membrane) of inner subfields by IOP. Error bars, 95% confidence interval. C, Graph showing the mean RPE thickness (including Bruch's membrane) of outer subfields by IOP. Error bars, 95% confidence interval.

Table 2. Mean Central Retinal Pigment Epithelium–Bruch’s Membrane Complex Thickness at Subfields by Smoking Status

Subfield and Smoking Status	Mean	95% Confidence Interval	P Value
Central			
No	26.47	26.4–26.53	Reference
Former smoker	26.11	26.02–26.19	<0.001
Yes, occasional	26.5	26.21–26.78	0.83
Yes, most or all days	26.36	26.17–26.55	0.32
Inner temporal			
No	26.11	26.05–26.17	Reference
Former smoker	26.02	25.95–26.1	0.07
Yes, occasional	26.23	25.98–26.48	0.38
Yes, most or all days	26.39	26.22–26.56	0.003
Inner superior			
No	24.57	24.51–24.63	Reference
Former smoker	24.38	24.3–24.45	<0.001
Yes, occasional	24.72	24.47–24.97	0.25
Yes, most or all days	24.63	24.46–24.8	0.5
Inner nasal			
No	27.15	27.09–27.21	Reference
Former smoker	27.04	26.97–27.12	0.02
Yes, occasional	27.18	26.92–27.45	0.81
Yes, most or all days	27.16	26.99–27.34	0.89
Inner inferior			
No	24.74	24.68–24.8	Reference
Former smoker	24.52	24.45–24.6	<0.001
Yes, occasional	24.83	24.57–25.08	0.52
Yes, most or all days	24.79	24.62–24.97	0.58
Outer temporal			
No	25.57	25.52–25.62	Reference
Former smoker	25.61	25.55–25.67	0.3
Yes, occasional	25.9	25.69–26.12	<0.001
Yes, most or all days	26.09	25.94–26.24	<0.001
Outer superior			
No	24.33	24.29–24.37	Reference
Former smoker	24.24	24.19–24.29	0.01
Yes, occasional	24.55	24.38–24.73	0.02
Yes, most or all days	24.47	24.34–24.59	0.04
Outer nasal			
No	26.84	26.79–26.89	Reference
Former smoker	26.83	26.76–26.89	0.73
Yes, occasional	27.2	26.97–27.43	<0.001
Yes, most or all days	27.13	26.98–27.29	<0.001
Outer inferior			
No	23.98	23.95–24.02	Reference
Former smoker	23.91	23.86–23.96	0.02
Yes, occasional	24.3	24.13–24.47	<0.001
Yes, most or all days	24.17	24.06–24.29	<0.001

Refraction was notable in that there seemed to be a trend toward a thicker RPE–BM complex with each 1-D increase in refraction (Fig 5; Table S2, available at www.aaajournal.org). This effect may be explained partially by ethnic differences in refraction, as Figure 6 demonstrates. Nevertheless, the effect persists in multivariate modeling, with RPE–BM complex thickness increasing 0.28 to 0.40 μm per 1-D increase in hyperopic refraction (or each decrease in myopic refraction; Table 3). A recent meta-analysis has attempted to identify associations between refractive error and macular degeneration, but any association appears weak.²³

Our study also showed that higher IOP is associated with thinning of the RPE–BM complex (Fig 7). Multivariate

Table 3. Multivariate Regression of Central Retinal Pigment Epithelium–Bruch’s Membrane Complex Thickness for Those 45 Years of Age and Younger versus Those Older Than 45 Years of Age

Age Group	Coefficient	95% Confidence Interval	P Value
45 yrs and younger			
Age (per yr)	0.02	–0.09 to 0.12	0.75
Women (vs. men)	–0.32	–0.73 to 0.10	0.13
Height (per cm)	–0.02	–0.05 to 0.00	0.03
Race (vs. white)			
Chinese	–0.84	–3.02 to 1.34	0.45
Asian	–0.12	–0.76 to 0.53	0.72
Black	3.61	2.95–4.27	<0.001
Mixed/other	1.77	0.95–2.59	<0.001
Refraction (per D)	0.40	0.3–0.50	<0.001
IOP _G (per mmHg)	–0.04	–0.08 to 0.01	0.14
Smoking status (vs. no)			
Former	–0.09	–0.43 to 0.26	0.62
Occasional	–0.40	–1.10 to 0.30	0.27
Yes, most or all days	–0.37	–0.9 to 0.17	0.18
Older than 45 yrs			
Age (per yr)	–0.10	–0.11 to –0.09	<0.001
Women (vs. men)	0.06	–0.09 to 0.21	0.41
Height (per cm)	–0.02	–0.03 to –0.02	<0.001
Race (vs. white)			
Chinese	–0.18	–1.06 to 0.71	0.70
Asian	–0.45	–0.82 to –0.08	0.02
Black	3.26	2.88–3.63	<0.001
Mixed/other	0.75	0.35–1.15	<0.001
Refraction (per 1 D)	0.28	0.25–0.31	<0.001
IOP (per mmHg)	–0.03	–0.05 to –0.02	<0.001
Smoking status (vs. no)			
Former	–0.10	–0.21 to 0.00	0.06
Occasional	–0.20	–0.52 to 0.12	0.22
Yes, most or all days	–0.27	–0.48 to –0.05	0.02

D = diopter; IOP = intraocular pressure; IOP_G = Goldmann-corrected intraocular pressure.

regression modeling suggested that this effect is not significant until after 45 years of age (Table 3) and is small and that the clinical significance is unknown. Nevertheless, this is a new and unexpected finding because there have been no reported associations between RPE–BM complex thickness and IOP and warrants further investigation.

The relationship with smoking is complex and must be interpreted with care, given the potential for underreporting of this habit by participants. Among those older than 45 years of age, regular smokers showed significantly thinner central RPE–BM complex as compared with nonsmokers (difference, –0.27 μm ; $P = 0.02$; Table 3). Many studies have attempted to link smoking with oxidative stress and damage to the RPE.^{24–26} Our findings suggest a locally mediated toxic effect of cigarette-derived compounds in the induction of RPE damage and subsequent loss. The finding that current smokers who classified themselves as regular smokers showed significantly thicker RPE–BM complexes as compared with nonsmokers in 5 of 9 subfields may be the result of accumulation of BM debris. In former smokers, a thicker RPE–BM complex most likely developed during their smoking years, but after cessation the debris was removed, resulting in a thinner RPE–BM

complex as found in our analysis. This would be one explanation for our findings, although alternatively, given the large number of measurements (more than 4 smoking classes and 9 subfields), the statistical finding of a thinner RPE–BM complex in former smokers simply may be the result of chance.

Given the large number of participants in this study, the negative findings are also important. There is no clinically significant association between RPE–BM complex thickness and systolic BP, diastolic BP, or BMI (Figs S3 and S4 and Tables S3 and S4, available at www.aaojournal.org). One may be misled by the small *P* values in regression analysis of individual variables; however, the slope of regressions is small, and the low *P* value likely represents the lack of fluctuation around a flat line.

Conclusions relating to RPE–BM complex thickness necessarily rely on interpretation of SD OCT imaging. We used optical reflectivity changes to identify inner and outer RPE boundaries and to infer changes in thickness. However, if optical reflectivity changes occur within the RPE cell for reasons other than shortening of cells, then there could be decoupling between optical reflectivity changes and true thickness change within the RPE–BM complex. Even if OCT-based measures of RPE–BM complex thickness are indeed valid, they may be the result of changes in structural, morphologic, and density indices. It is not possible to be certain of any direct relationship with function.

This study's strengths include its standardized methodology, the inclusion of multiple races and ethnicities across the United Kingdom, and the unprecedented number of high-quality SD OCT images of the macula. This study is limited in that UK Biobank is not population based, and thus people with fewer resources to attend community research sites are likely underrepresented. Despite these drawbacks, the UK Biobank resource represents an enormously valuable repository of data, and the present analysis is a source of both normative data and information on associations between ocular-level findings and other factors. In this analysis, we reported RPE–BM complex thickness values in normal participants and deliberately excluded eyes with poor-quality SD OCT images. We have no reason to suspect that RPE–BM complex thickness is significantly different in eyes with no disease but in which the scan quality was poor. However, because we excluded such scans from our analysis, we cannot be certain of the possibility of this approach resulting in unintentional bias with respect to RPE–BM complex thickness values. Also, the absolute values of RPE–BM complex thickness we found in this study are specific to the algorithm used for the analysis, and different values may be obtained using different segmentation algorithms.

In summary, we reported novel findings relating to RPE–BM complex thickness and showed that this layer varies by topography, age, gender, and race. We also observed notable associations with myopia, IOP, and smoking status. These findings suggest new directions of research to permit better understanding of the RPE–BM complex and its role in disease pathogenesis.

References

- Huang D, Swanson EA, Lin CP, et al. Optical coherence tomography. *Science*. 1991;254:1178-1181.
- Schuman JS, Pedut-Kloizman T, Hertzmark E, et al. Reproducibility of nerve fiber layer thickness measurements using optical coherence tomography. *Ophthalmology*. 1996;103:1889-1898.
- Cense B, Nassif N, Chen T, et al. Ultrahigh-resolution high-speed retinal imaging using spectral-domain optical coherence tomography. *Opt Express*. 2004;12:2435-2447.
- Nassif N, Cense B, Park B, et al. In vivo high-resolution video-rate spectral-domain optical coherence tomography of the human retina and optic nerve. *Opt Express*. 2004;12:367-376.
- Strauss O. The retinal pigment epithelium in visual function. *Physiol Rev*. 2005;85:845-881.
- Jonas JB. Global prevalence of age-related macular degeneration [Peer commentary on: "Global prevalence of age-related macular degeneration and disease burden projection for 2020 and 2040: a systematic review and meta-analysis." By Wong, WL, Su, X, Li, X, et al.] *Lancet Glob Health*. 2014;2:e65-e66.
- Friedman DS, O'Colmain BJ, Muñoz B, et al. Prevalence of age-related macular degeneration in the United States. *Arch Ophthalmol*. 2004;122:564-572.
- Munoz B, West SK, Rubin GS, et al. Causes of blindness and visual impairment in a population of older Americans: the Salisbury Eye Study. *Arch Ophthalmol*. 2000;118:819-825.
- Klaver CC, Wolfs RC, Vingerling JR, et al. Age-specific prevalence and causes of blindness and visual impairment in an older population: the Rotterdam Study. *Arch Ophthalmol*. 1998;116:653-658.
- Wang JJ, Foran S, Mitchell P. Age-specific prevalence and causes of bilateral and unilateral visual impairment in older Australians: the Blue Mountains Eye Study. *Clin Exp Ophthalmol*. 2000;28:268-273.
- Wing GL, Blanchard GC, Weiter JJ. The topography and age relationship of lipofuscin concentration in the retinal pigment epithelium. *Invest Ophthalmol Vis Sci*. 1978;17:601-607.
- Ach T, Zarubina AV, Hammack KM, et al. Quantified autofluorescence maps of human retinal pigment epithelium in age-related macular degeneration (AMD). *Invest Ophthalmol Vis Sci*. 2015;55:4832-4841.
- Ramrattan RS, van der Schaft TL, Mooy CM, et al. Morphometric analysis of Bruch's membrane, the choriocapillaris, and the choroid in aging. *Invest Ophthalmol Vis Sci*. 1994;35:2857-2864.
- Curcio CA, Messinger JD, Sloan KR, et al. Human chorioretinal layer thicknesses measured in macula-wide, high-resolution histologic sections. *Invest Ophthalmol Vis Sci*. 2011;52:3943-3954.
- Karampelas M, Sim DA, Keane PA, et al. Evaluation of retinal pigment epithelium–Bruch's membrane complex thickness in dry age-related macular degeneration using optical coherence tomography. *Br J Ophthalmol*. 2013;97:1256-1261.
- Farsiu S, Chiu SJ, O'Connell RV, et al. Quantitative classification of eyes with and without intermediate age-related macular degeneration using optical coherence tomography. *Ophthalmology*. 2014;121:162-172.
- Yang Q, Reisman CA, Wang Z, et al. Automated layer segmentation of macular OCT images using dual-scale gradient information. *Opt Express*. 2010;18:21293-21307.
- Starengi G, Sadda S, Chakravarthy U, et al. Proposed lexicon for anatomic landmarks in normal posterior segment

- spectral-domain optical coherence tomography: the IN•OCT consensus. *Ophthalmology*. 2014;121:1572-1578.
19. Patel PJ, Foster PJ, Grossi CM, et al. Spectral-domain optical coherence tomography imaging in 67,321 adults: associations with macular thickness in the UK Biobank Study. *Ophthalmology*. 2016;123:829-840.
 20. Demirkaya N, van Dijk HW, van Schuppen SM, et al. Effect of age on individual retinal layer thickness in normal eyes as measured with spectral-domain optical coherence tomography. *Invest Ophthalmol Vis Sci*. 2013;54:4934-4940.
 21. Grossniklaus H, Kang S, Zhang Q. In vivo contrast-enhanced high-frequency ultrasonography of experimental uveal melanoma: imaging features and histopathologic correlations. *Invest Ophthalmol Vis Sci*. 2013;54:4229.
 22. Wong WL, Su X, Li X, et al. Global prevalence of age-related macular degeneration and disease burden projection for 2020 and 2040: a systematic review and meta-analysis. *Lancet Glob Health [serial online]*. 2014;2:e106-e116. Accessed January 27, 2016; [http://www.thelancet.com/journals/langlo/article/PIIS2214-109X\(13\)70163-3/fulltext](http://www.thelancet.com/journals/langlo/article/PIIS2214-109X(13)70163-3/fulltext).
 23. Li Y, Wang J, Zhong X, et al. Refractive error and risk of early or late age-related macular degeneration: a systematic review and meta-analysis. *PLoS One*. 2014;9:e90897. Accessed January 27, 2016; <http://journals.plos.org/plosone/article?id=10.1371/journal.pone.0090897>.
 24. Liang FQ, Godley BF. Oxidative stress-induced mitochondrial DNA damage in human retinal pigment epithelial cells: a possible mechanism for RPE aging and age-related macular degeneration. *Exp Eye Res*. 2003;76:397-403.
 25. Kunchithapautham K, Atkinson C, Rohrer B. Smoke exposure causes endoplasmic reticulum stress and lipid accumulation in retinal pigment epithelium through oxidative stress and complement activation. *J Biol Chem*. 2014;289:14534-14546.
 26. Woodell A, Rohrer B. A mechanistic review of cigarette smoke and age-related macular degeneration. *Adv Exp Med Biol*. 2014;801:301-307.

Footnotes and Financial Disclosures

Originally received: March 23, 2016.

Final revision: June 29, 2016.

Accepted: July 22, 2016.

Available online: ■■■■.

Manuscript no. 2016-608.

¹ NIHR Biomedical Research Centre at Moorfields Eye Hospital NHS Foundation Trust and UCL Institute of Ophthalmology, University College London, London, United Kingdom.

² Topcon Advanced Biomedical Imaging Laboratory, Oakland, New Jersey.

³ Optometry & Vision Science, Queens University of Belfast, Belfast, United Kingdom.

⁴ Department of Ophthalmology, Southampton General Hospital, Hampshire, United Kingdom.

*A full list of the UK Biobank Eye & Vision Consortium study group is available online (www.aaojournal.org).

Financial Disclosure(s):

The author(s) have made the following disclosure(s): P.J.F.: Consultant – Zeiss (Oberkochen, Germany) Financial support – Alcon (Fort Worth, TX); Allergan (Marlow, Buckinghamshire, UK); Lecturer – Allergan; Board membership – Allergan; Expert testimony – Alcon, Allergan, Zeiss. N.G.S.: Lecturer – Allergan; Alcon; Novartis (Camberley, Surrey, UK); Heidelberg Engineering (Hemel Hempstead, Hertfordshire, UK); Financial support – Allergan

Q.Y.: Employee – Topcon Medical Systems, Inc (Tokyo, Japan)

C.A.R.: Employee – Topcon Medical Systems, Inc.

U.C.: Consultant – Novartis; Bayer; Allergan; Roche (Basel, Switzerland); Financial support (to institution) – Roche

P.A.K.: Lecturer – Allergan; Novartis; Bayer (Leverkusen, Germany); Topcon; Heidelberg; Financial support – Allergan

P.J.P.: Consultant – Thrombogenics (to institution) (Leuven, Belgium); Bayer; Novartis; Merck (Kenilworth, NJ); Financial support – Bayer UK (Newbury, Berkshire, UK); Bayer; Salutaris MD (Tuscan, AZ); Lecturer – Bayer; Heidelberg Engineering; Topcon; Allergan; Alcon

The UK Biobank was established by the Wellcome Trust (London, UK), medical charity; the Medical Research Council (London, UK); the Department of Health (London, UK); Scottish Government (Edinburgh, UK); and the Northwest Regional Development Agency (Warrington, UK). It also received funding from the Welsh Assembly Government (Cardiff, UK); the British Heart Foundation (London, UK); and Diabetes UK (London, UK). Supported by the Richard Desmond Charitable Trust (London, UK) via Fight for Sight (London, UK) (grant no.: 1956 [P.J.F.]); the Special Trustees of Moorfields Eye Hospital, London, United Kingdom (grant no.: ST 12 09); and the Department for Health through the award made by the NIHR Biomedical Research Centre at Moorfields Eye Hospital NHS Foundation Trust, London, United Kingdom (grant no.: BRC2_009). The funding organizations had no role in the design or conduct of this research.

Presented at the Association for Research in Vision and Ophthalmology (ARVO) Annual Meeting 2016 in Seattle, Washington.

Author Contributions:

Conception and design: Foster, Patel, Ko

Analysis and interpretation: Ko, Foster, Patel, Strouthidis, Shweikh, Yang, Reisman, Muthy, Chakravarthy, Lotery, Keane, Tufail, Grossi

Data collection: Foster, Patel, Ko, Reisman, Yang

Obtained funding: Foster, Patel, Strouthidis, Ko

Overall responsibility: Patel, Foster, Ko

Abbreviations and Acronyms:

BM = Bruch's membrane; **BMI** = body mass index; **BP** = blood pressure; **CI** = confidence interval; **D** = diopter; **ETDRS** = Early Treatment of Diabetic Retinopathy Study; **ILM** = internal limiting membrane; **IOP** = intraocular pressure; **NFL** = nerve fiber layer; **OCT** = optical coherence tomography; **RPE** = retinal pigment epithelium; **SD** = standard deviation; **SE** = standard error; **TABS** = Topcon Advanced Boundary Segmentation.

Correspondence:

Praveen J. Patel, MD, FRCOphth, Moorfields Eye Hospital NHS Foundation Trust, 162 City Road, London EC1V 2PD, United Kingdom.

E-mail: praveen.patel@moorfields.nhs.uk.